Materials Chemistry and Physics xxx (2015) 1–9

Contents lists available at ScienceDirect

Materials Chemistry and Physics

journal homepage: www.elsevier.com/locate/matchemphys

Thermomechanical response and toughening mechanisms of a carbon nano bead reinforced epoxy composite

M.S. Goyat [a, *], Sumit Suresh [a], Sumit Bahl [a], Sudipta Halder [b], P.K. Ghosh [a]

[a] Department of Metallurgical and Materials Engineering, Indian Institute of Technology Roorkee, Roorkee, 247667, India
[b] Department of Mechanical Engineering, National Institute of Technology, Silchar, 788010, Assam, India

HIGHLIGHTS

- Synthesis of uniform size, spherical CNB using chemical vapour deposition method.
- Fabrication of CNB/epoxy nanocomposites by ultrasonic dual mode mixing route.
- Significant enhancement in thermomechanical properties of CNB/epoxy nanocomposite.
- Main toughening mechanisms: Crack deflection, particle bridging and shear yielding.

ARTICLE INFO

Article history:
Received 10 July 2015
Received in revised form
22 August 2015
Accepted 20 September 2015
Available online xxx

Keywords:
Composite materials
Thermogravimetric analysis (TGA)
Electron microscopy (FESEM)
Mechanical properties
Thermal properties

ABSTRACT

The current research on carbon nano beads (CNB) is focused on various applications such as high strength nanocomposites, electronic devices, lubricants, semiconductors, and high-performance batteries, etc. The commercial uses of CNB are yet juvenile for the market. Only limited results have been published so far on CNB reinforced polymers [1]. This study highlights the synthesis of uniform size, spherical CNB using chemical vapour deposition (CVD) method. The synthesized CNB are introduced into epoxy matrix by ultrasonic dual mode mixing route to produce CNB/epoxy nanocomposite. The CNB are characterized by X-ray diffraction, Energy dispersive X-ray analysis and field emission scanning electron microscope (FESEM). Morphology, thermal and mechanical properties of the CNB/epoxy nanocomposites is characterized by FESEM, Thermo-gravimetric analyzer and tensile and bending tests respectively. A noticeable improvement in thermal and mechanical properties of CNB reinforced epoxy matrix with low nanofiller content is observed. Several toughening mechanisms such as particle pull out, crack deflection, particle bridging, crack pinning, shear yielding or plastic deformation, and microcracking are identified. But, only the crack deflection, particle bridging and shear yielding or plastic deformations are recognized as the leading toughening mechanisms for CNB/epoxy nanocomposite. These results can be considered as symptomatic of a potential CNB espousal in new composites.

1. Introduction

Over the past few decades lots of research has been performed worldwide to reinforce polymeric materials with various types of micro-fillers and nanofillers to enhance their thermal, mechanical and electrical properties for diverse engineering applications [2–9]. The micro-fillers that have been explored include Al_2O_3, Al, and Cu etc., [10]. Similarly, the investigated nanofillers include Al_2O_3, TiO_2, SiO_2, ZrO_2 nanoparticles [11–14], carbon nanotubes [4], nanoclays [5,6] and more recently graphene, etc., [7–9]. The superiority of nanofillers over micro-fillers is well known. The nanofillers especially carbon nanostructures have a great potential to improve thermal stability, mechanical properties like strength, modulus, toughness, wear, creep and fatigue resistance, etc. Although the carbon nanotubes (CNTs) constitute a well-known material for improving the mechanical properties of the polymers, but the cross-linking density of epoxy matrix is seriously hampered due to incorporation of high aspect ratio CNTs especially beyond 1 wt% [15]. But, the addition of spherical nanoparticles (which offers less hindrance to the cross-linking density of epoxy due to their low aspect ratio ~1) beyond 10 wt% is found quite effective for

* Corresponding author. Present address: Department of Physics, University of Petroleum & Energy Studies, Dehradun, 248007, Uttarakhand, India.
E-mail address: goyatmanjeetsingh@gmail.com (M.S. Goyat).

http://dx.doi.org/10.1016/j.matchemphys.2015.09.038
0254-0584/

improvement in mechanical and thermal properties of the polymers [3,11–13]. Over the past two decades various shaped carbon nanomaterials have been synthesized, characterized and studied in different environments. Though carbon spheres have been identified for decades, but the investigation on synthesis of spherical shaped carbon has turned out to be newsworthy in last few years. These spherical shaped carbon materials have been denoted as nanosized carbon spheres [1,16–18], carbon nano beads [19–21], carbon spherules [22] and nano balls [23], etc. The interest in synthesis of carbon nano spheres relates to their high conductivity, thermal stability, strength and lightweight. These carbon nano spheres also have been used in high strength composites, catalyst carriers, lubricants, electronic devices [1,24–26].

In view of the above, an attempt has been made to synthesize carbon nano beads in order to tune the thermal and mechanical properties of the epoxy matrix. In the present study, the incorporation of CNB in epoxy matrix leads to the significant improvement in thermal stability, tensile and fracture properties of the epoxy composite at very low nanofiller content (2 wt%). Several toughening mechanisms are identified and discussed for organic particulate filled thermosetting polymers. These results suggest that CNB illustrate momentous potential as a reinforcing ingredient in polymeric composites.

2. Experimental

2.1. Materials

Cobalt (II) acetate tetrahydrate, citric acid monohydrate and nitric acid were procured from SIGMA–ALDRICH, India. Two component epoxy paste adhesive: Araldite AW 106 Resin/Hardener HV 953U was purchased from Huntsman Advanced Materials Americas Inc., USA.

2.2. Synthesis of carbon nano beads (CNB)

Metal containing catalysts were synthesized by aqueous sol–gel method. 2.365 g of citric acid monohydrate and 10 g of cobalt (II) acetate were blended while stirring gently at a gelation temperature ~80 °C till the formation of a gel. The gel was dried in an oven at 120 °C for 6 h and then calcined in air for 5 h at 350 °C. The calcined sample was converted to fine powder (catalyst) using pestle and mortar. Alumina boat containing catalyst was placed in a tubular furnace at 600 °C under ammonia gas flowing at a rate of 60 sccm and then temperature was increased to 630 °C at a heating rate of 8 °C/min before passing acetylene gas with ammonia gas for 10 min at a flow rate of 20 sccm for growing carbon nano structures (CNS). The CNS were dispersed in nitric acid solution (6 M HNO_3) using ultrasonic bath followed by addition of double distilled (DD) water and kept at ambient conditions for 48 h, including continuous removal of floating waste in the suspension (CNS settle down at the bottom) and again diluting it with DD water until its pH value reaches ~7. Then the suspension was kept in an oven at 40 °C till its complete drying.

2.3. Solution-blended CNB/epoxy nanocomposites

Four times volume of methyl ethyl ketone (MEK) was blended with epoxy resin using magnetic stirring. Varying amount of 0.5, 1, 2 and 3 wt% of CNB was blended with mixture of epoxy resin and MEK using optimized ultrasonic dual mode mixing (UDMM) process. The choice of optimized UDMM is based on our previous result [13]. Ultrasonic cavitation by a Vibracell ultrasonic processor (Sonics & Materials, Inc.) along with magnetic stirring was employed to prepare CNB/epoxy nanocomposites. After the UDMM process for 1 h, the MEK was removed under high vacuum of 1.33×10^{-4} to 1.33×10^{-5} bars for 2 h, and the well dispersed blend was cooled to room temperature (23 °C). The removal of MEK was confirmed by following a method described in our earlier work [11]. Hardener was mixed in a stoichiometric ratio to the well dispersed blend. Then, glass rod stirring was employed for 10 min followed by degassing at room temperature to remove the entrapped air. The resulting composite was poured into molds and allowed to cure in hot air oven for 16 h at 40 °C.

3. Characterizations

3.1. Spectroscopic analysis

The dried carbonaceous material was characterized using X-ray diffractometer (XRD) (Bruker D8 Advance Diffractometer, Germany) with operating voltage of 40 kV and current of 40 mA, under Cu-Kα radiation having wavelength 1.54 Å. A dwell time of 2 s per step was used. The elemental analysis of carbonaceous material was performed using energy dispersive X-ray analysis (EDAX). The samples were plasma coated with a thin layer of gold ~6 nm for electrical conduction and to reduce the surface charging during analysis.

3.2. Morphology of CNB and CNB/epoxy nanocomposites

Morphology of CNB was observed by field-emission scanning electron microscope (FESEM) Quanta 200F (FEI, USA) with accelerating voltage of 20 kV and working distance of ~10 mm. The dispersion of CNB in the epoxy matrix and tensile test specimen's fracture surfaces were studied by FESEM with accelerating voltage of 15 kV to avoid the degradation of polymer material during analysis. The samples were plasma coated with a thin layer of gold ~6 nm for electrical conduction.

3.3. Thermo-gravimetric (TG) analysis

The TG analysis was carried out with Perkin–Elmer thermal analyzer (Pyris Diamond, TG/DTG, USA). Alumina powder was used as a reference material and the initial sample mass was 10 mg. All measurements were performed under a nitrogen atmosphere (200 ml/min nitrogen flow) from room temperature to 700 °C at a heating rate of 10 °C/min. Thermal stability was determined using TG and differential thermo-gravimetric (DTG) curves. Data reported in this study is an average of at least 3 measurements with samples from different batches.

3.4. Tensile testing

Tensile testing of CNB/epoxy nanocomposites was carried out following the ASTM D-638(V) standard [14]. Dumbbell-shaped tensile specimens of size 63.5 mm × 10 mm × 3.2 mm (length, width and thickness) were tested by a computer controlled universal tester H25KS (Tinius Olsen, India) with 25 kN load cell at a crosshead speed of 1 mm/min. The stress–strain curves of the tensile test specimens were used for determination of tensile strength, elastic modulus and strain-to-break% [14]. The room temperature was 23 °C and the relative humidity was 57.3%. Data reported in this study is an average of at least 3 measurements with samples from different batches.

3.5. Bending testing

Fracture toughness and fracture energy was measured as per ASTM D5045 standard. Single-edge-notch 3-point bending test

Please cite this article in press as: M.S. Goyat, et al., Thermomechanical response and toughening mechanisms of a carbon nano bead reinforced epoxy composite, Materials Chemistry and Physics (2015), http://dx.doi.org/10.1016/j.matchemphys.2015.09.038

specimens of size 55 mm × 12.5 mm × 6.25 mm (length, width and thickness) were tested using a computer controlled universal tester H25KS (Tinius Olsen, India) with 25 kN load cell at a crosshead speed of 10 mm/min. The temperature was 23 °C and the relative humidity was 57.3%. Data reported in this study is an average of at least 3 measurements with samples from different batches.

4. Results and discussion

4.1. Spectroscopic investigation

The wide angle X-ray diffraction pattern of carbonaceous material is shown in Fig. 1(a). The pattern reveals two broad peaks at 26.6° and 43.3°, which corresponds to partial crystalline nature of small size carbon beads. The peak at 26.6° matches with an interlayer d-spacing of ~0.33 nm, which indicates the ordering of carbon plane and is in good agreement with graphitic nature of carbon [27].

The EDAX spectrum as shown in Fig. 1(b) indicates the presence of C, O and Au elements in the carbonaceous material. Where, the presence of Au is due to gold coating on sample. The presence of 95.56 wt% (98.90 At.%) of C indicates the formation of carbon nano structure. The very small content of oxygen about 1.15 wt% may promote the clustering of the nanostructures and also it may slightly reduce the reinforcing effect of the nanostructures in epoxy matrix.

4.2. Morphology of CNB, and CNB/epoxy nanocomposites

Fig. 2(a) and (b) reveals a large number of uniform and almost spherical CNB of diameter about 80–90 nm with smooth surface. The CNB grow like a chain. The CNB of almost equivalent sizes are interconnected with each other in random fashion to form agglomerated carbon clusters.

Good dispersion of nanoparticles in polymeric matrix plays a vital role to take the advantage of nanoscale particles in order to achieve enhanced properties. The number and agglomerate size of carbon particles may increase with the increasing particle content. Fig. 3 shows the dispersion of 2 wt% CNB/epoxy nanocomposite. Fig. 3(a) reveals a noticeable amount of clustering of nano beads in epoxy matrix, while the comparatively magnified image of FESEM as shown in Fig. 3(b) reveals most of the nano beads are individually dispersed except few agglomerates. Further addition of nano beads (3 wt%) in epoxy matrix leads to a significant clustering of beads which is not shown here. This may be attributed to the strong interaction of carbon–carbon spheres. It infers that the optimized UDMM does not provide enough energy so that it can break up all strong inter-connected carbon–carbon particles. This becomes even more challenging if the content of carbon particles increased from 2 to 3 wt%.

4.3. Thermal properties

The characteristic TGA plots of neat epoxy and CNB/epoxy nanocomposites are shown in Fig. 4. The initial decomposition temperature (IDT), maximum decomposition temperature (MDT) and characteristic yield percentage (CYP) of the nanocomposites has been measured using the TGA curves (Fig. 4) and are shown in Fig. 5. The IDT steadily increases with the increase of CNB content in epoxy. The increase of IDT is an indicative of homogeneous dispersion of CNB in epoxy matrix, which may act as obstacles to heat flow through the matrix [11]. The presence of CNB in the epoxy matrix may delay the predominant random chain scission of the epoxy matrix [28] and also results in the delay of the initial step of thermal degradation. However, the MDT increases with the increase of CNB content up to 2 wt% and is followed by a slight decrease in it for 3 wt% of CNB. A slight decrease in MDT of 3 wt% CNB/epoxy nanocomposite compared to 2 wt% CNB/epoxy nanocomposite may be due to the non-homogeneous dispersion of CNB in epoxy matrix for higher content of particles. The CYP depicts the change in the weight % of neat epoxy and CNB/epoxy nanocomposites at 700 °C. Since CNB does not decompose at 700 °C, the final weight should increase with the increasing CNB content while the stoichiometry of the epoxy matrix was maintained [29]. Therefore, the CYP of nanocomposite increases with the increase of CNB content up to 2 wt%. But, the CYP in case of 3 wt% CNB/epoxy nanocomposite decreases and this decrease endorses the non-stoichiometry of the epoxy matrix.

In general, the degradation of epoxy network occurs in a two stages. The first stage occurs at the temperature between 35 °C and 310 °C, which is ascribed to the evaporation of residual solvent and adsorbed humidity [30]. The second stage takes place from 310 °C to 450 °C, which is ascribed to the thermal degradation of the cured epoxy network [30]. Mostly, the incorporation of foreign particles in epoxy reduces its cross-linking density to some extent especially when the particle content is high and particles are not dispersed homogeneously. The reduction in cross-linking density results in lower decomposition temperature [29]. Similar to the neat epoxy, the nanocomposites revealed two-stage degradation in DTG plots as shown in Fig. 6. However, for the nanocomposites, temperature at maximum rate of mass loss highlighted by dotted line is enhanced with respect to neat epoxy and also the formation of residue is obviously increased.

4.4. Mechanical properties

Tensile stress vs strain curves for neat epoxy and CNB/epoxy nanocomposites with CNB content ranging from 0.5 to 3 wt% are shown in Fig. 7. The effect of CNB content on ultimate tensile strength, Young's modulus and strain-to-break% of the resulting

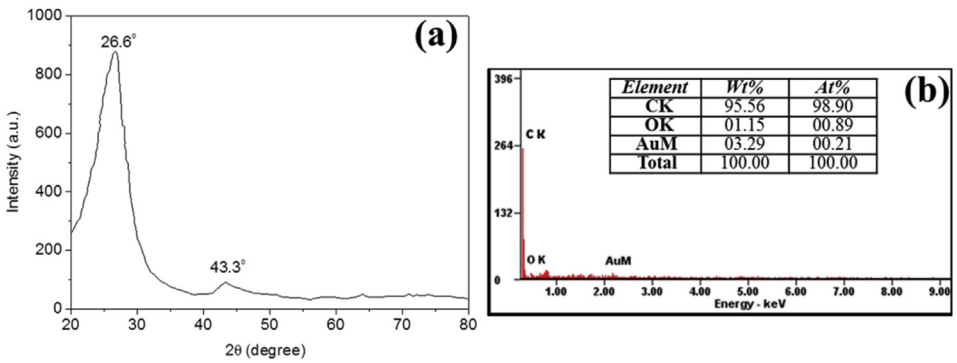

Fig. 1. (a) XRD pattern of carbon nano beads and (b) EDAX spectrum of carbon nano beads.

Please cite this article in press as: M.S. Goyat, et al., Thermomechanical response and toughening mechanisms of a carbon nano bead reinforced epoxy composite, Materials Chemistry and Physics (2015), http://dx.doi.org/10.1016/j.matchemphys.2015.09.038

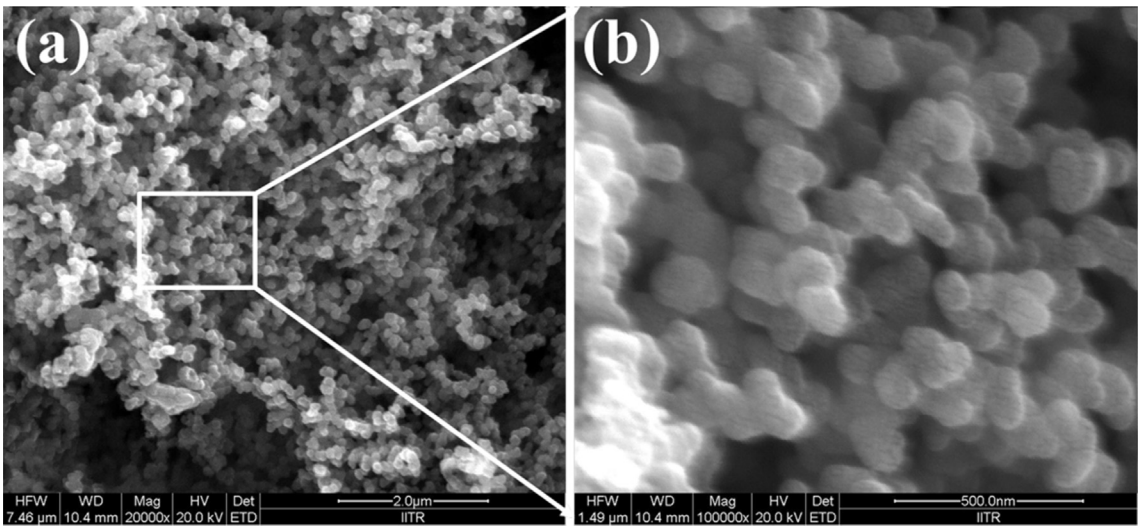

Fig. 2. FESEM images of CNB at (a) lower and (b) higher magnification.

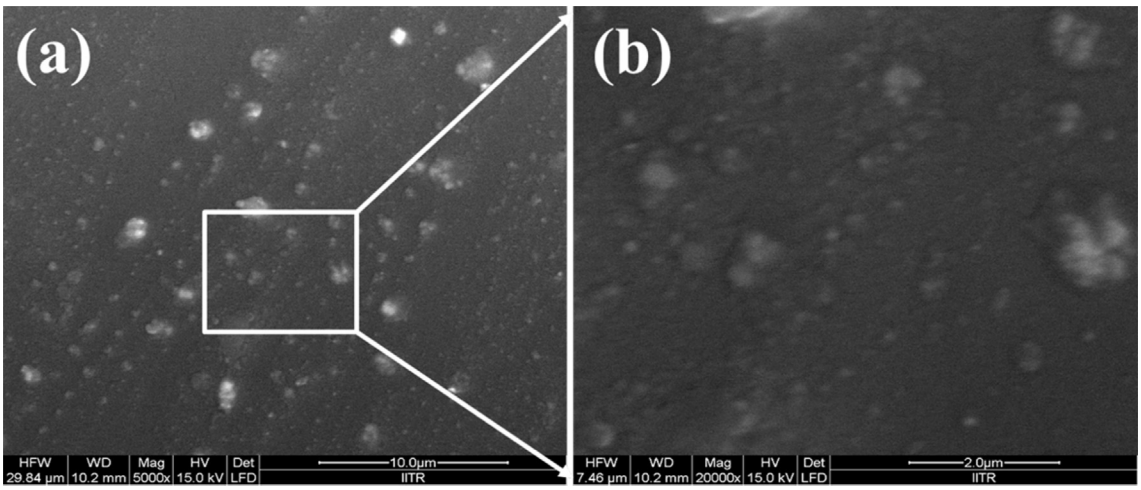

Fig. 3. FESEM images of 2 wt% CNB/epoxy nanocomposite at (a) lower and (b) higher magnification.

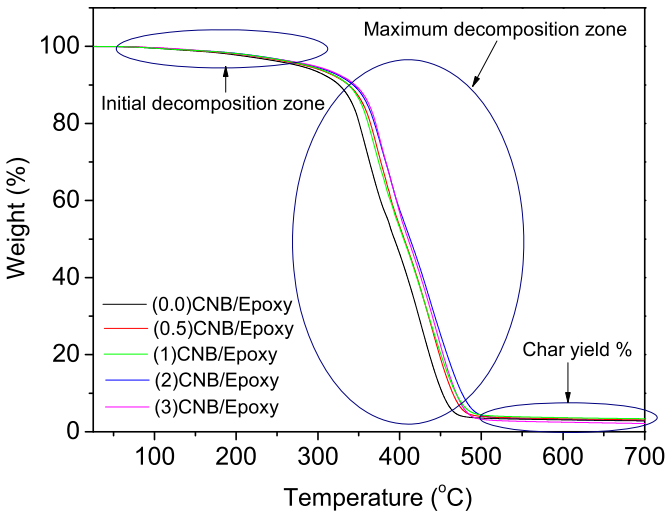

Fig. 4. TGA plots of CNB/epoxy nanocomposites.

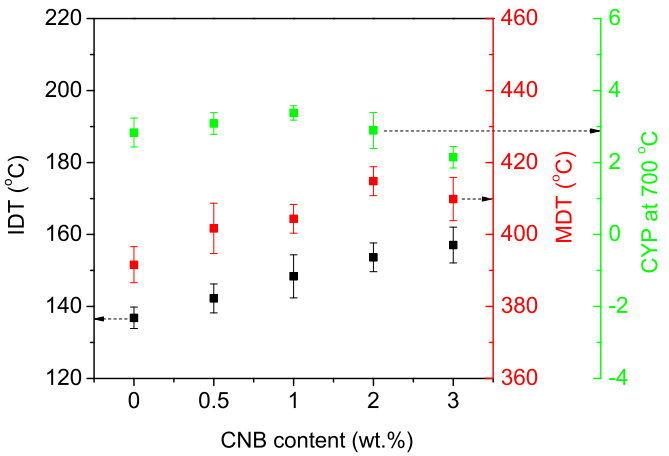

Fig. 5. Trend of initial decomposition temperature (IDT), maximum decomposition temperature (MDT) and characteristic yield percentage (CYP) of CNB/epoxy nanocomposites with respect to CNB content.

Please cite this article in press as: M.S. Goyat, et al., Thermomechanical response and toughening mechanisms of a carbon nano bead reinforced epoxy composite, Materials Chemistry and Physics (2015), http://dx.doi.org/10.1016/j.matchemphys.2015.09.038

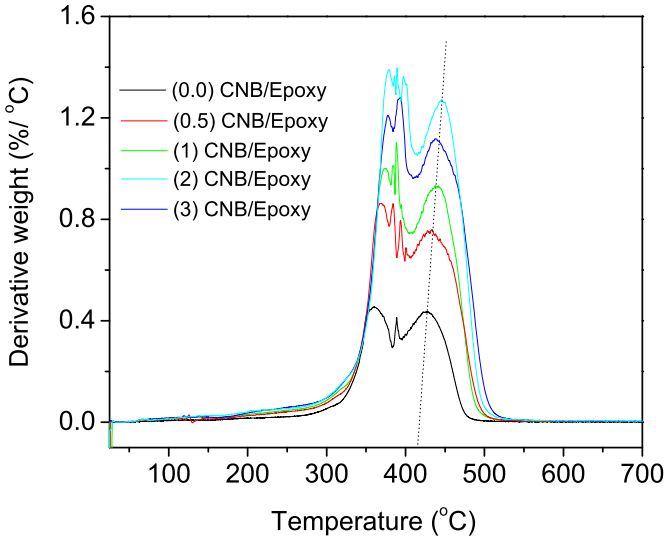

Fig. 6. DTG plots of CNB/epoxy nanocomposites.

nanocomposites is shown in Fig. 8, where the error bars denote the maximum and minimum values. The addition of CNB is effective for increasing the tensile strength and modulus of the epoxy at low nanofiller loading (0.5–2 wt%). But, beyond 2 wt% loading, a decline in performance is observed but it is still better than that of the neat epoxy. The maximum enhancement in tensile strength and modulus (~25% and ~47% respectively at 2 wt% of CNB) is impressive. The strain-to-break% gradually decreases with the increase of CNB content in epoxy, which means the flexibility of the matrix, is compromised at the cost of enhancement in strength. The maximum decrease in strain-to-break% is ~21%.

The effect of CNB content on fracture toughness (K_{Ic}) and fracture energy (G_{Ic}) of the nanocomposites is shown in Fig. 9, where the error bars denote the maximum and minimum values. The K_{Ic} of neat epoxy is ~0.53 MPa $m^{1/2}$. The addition of CNB into the epoxy results in an increase in K_{Ic} value to ~0.79 MPa $m^{1/2}$ at ~2 wt% of CNB, which corresponds to a ~49% increase in fracture toughness, which is quite interesting. For higher CNB content (3 wt%), the improvement in K_{Ic} reduces to ~0.69 MPa $m^{1/2}$, but it is still higher than that of the base matrix. To attain analogous percentage of

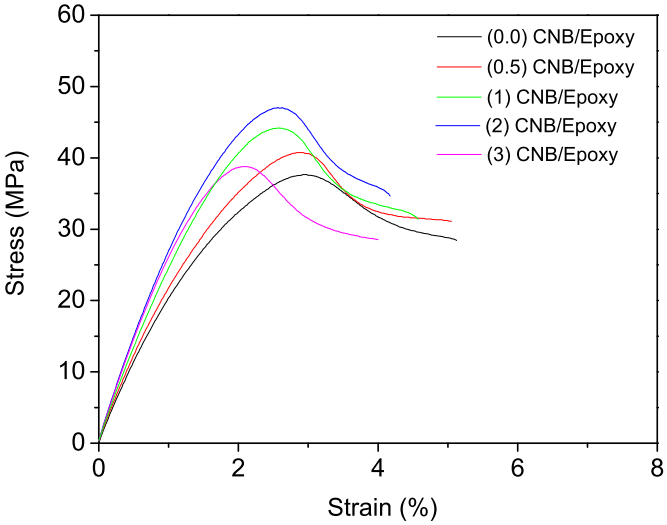

Fig. 7. Quasi-static stress vs strain profile of CNB/epoxy nanocomposites.

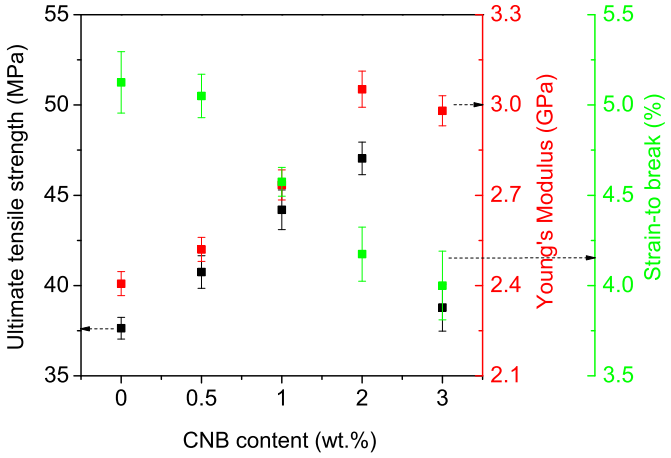

Fig. 8. Tensile properties of the CNB/epoxy nanocomposites: Ultimate tensile strength vs CNB content, Young's modulus vs CNB content and Strain-to-break% vs CNB content.

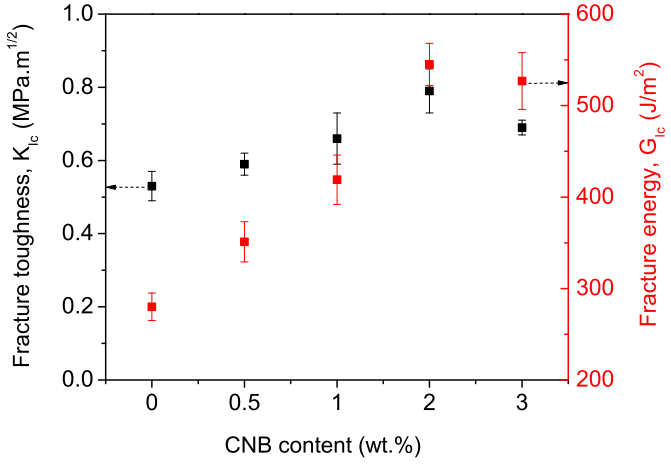

Fig. 9. 3-point bending fracture properties of the CNB/epoxy nanocomposites: Mode I fracture toughness vs CNB content and Mode I fracture energy vs CNB content.

enhancement (~49%) in K_{Ic}, the required wt% of silica nanoparticles in epoxy matrix was found greater than 10 wt% [2] which is 5-fold greater than for CNB. Similarly, to obtain a 49% increase in K_{Ic}, the loading content of alumina (5%) and titania (10%) nanoparticles [2] in epoxy is ~2 to 10-fold greater than CNB.

The fracture energy of the nanocomposite has been calculated with the help of following relation: $G_{Ic} = K_{Ic}^2[(1-\mu^2)/E]$, where μ is Poisson's ratio [9]. The fracture energy (G_{Ic}) enumerates the energy required for crack propagation in a material. The calculated G_{Ic} of neat epoxy is 280 J/m^2. Addition of CNB into the epoxy results in a significant increase in G_{Ic} of the nanocomposite to 545 J/m^2 at 2 wt % of CNB. However, further addition of CNB to 3 wt% leads to a decline in the fracture energy of the nanocomposite. The maximum enhancement in the fracture energy of CNB/epoxy nanocomposite is ~95% at 2 wt% of CNB. This noticeable enhanced energy release rate of the CNB/epoxy nanocomposite material is comparable with tough polymers [31]. These results exhibit the potential of CNB in toughening the epoxy polymer at very low nanofiller content (2 wt %). A consistent tendency demonstrated in the results for tensile strength, elastic modulus, fracture toughness, fracture energy and fracture surface roughness is that the CNB fillers quickly lose efficiency beyond a loading content of 2 wt%. This is happening due to clustering of CNB. Because, the CNB agglomeration aids to diminish the interfacial contact area at CNB/epoxy matrix interface and

Please cite this article in press as: M.S. Goyat, et al., Thermomechanical response and toughening mechanisms of a carbon nano bead reinforced epoxy composite, Materials Chemistry and Physics (2015), http://dx.doi.org/10.1016/j.matchemphys.2015.09.038

hence, it weakens the ability of the CNB to reinforce the composite. The clustering of CNB leads to poor interaction between the nanofiller and epoxy matrix. The clusters of CNB can act as defect centers in the epoxy matrix causing a detrimental effect on the mechanical properties.

4.5. Fracture mechanisms

Numerous mechanisms for energy dissipation are well-known and accepted for thermosetting polymers and particulate filled thermosetting polymers [3]. Some of the known extrinsic toughening mechanisms contributing in inorganic nanoparticles-modified epoxy are particle pull out, crack deflection, particle bridging, crack pinning, shear yielding or plastic deformation, and microcracking [3]. All these known reinforcing mechanisms are scrutinized and discussed for CNB/epoxy nanocomposites in the following sub-sections.

Most commonly, three different fracture zones observed in case of thermosetting polymers such as (i) mirror, (ii) mist and (iii) hackle [31] on the tensile fracture surfaces. All these fracture zones can be easily seen on the tensile fracture surfaces of 2 wt% CNB/epoxy nanocomposite as shown in Fig. 10(a). A crack nucleates at a minute flaw and propagates normal to the tensile axis. In initial stage of fracture, the crack grows very slowly and then accelerates which creates very smooth fracture surfaces known as the mirror zone [32] (shown by red color dashed semicircle and denoted by X). This fracture zone is surrounded by a little rougher and very thin region known as the mist zone (shown by yellow color dashed semicircle and denoted by Y). A very rough and thick region, surrounding the mist zone is known as hackle zone (denoted by Z), which forms when the crack reached its fastest speed and excess stored energy dissipates in form of bifurcation [32]. A magnified FESEM image of the mirror zone of nanocomposite (Fig. 10(b)) is showing formation of crazes, which is a basic characteristic of a thermosetting polymer.

4.5.1. Particle pull-out

Particle pull-out occurs due to debonding between the nanoparticles and epoxy matrix, which creates almost hemi-spherical holes or nanocavities on the fracture surface [33]. Usually, any debonding phenomenon in the mirror or hackle zone is expected to increase the resistance to the crack propagation [34]. This mechanism is reported for weak nanoparticle−matrix interface in the literature [33], which can be explained as the crack propagation at very low velocity in the mirror zone results in debonding in fracture surface morphology. This mechanism (indicated by 'A') hardly appears in the mirror and hackle zone of the CNB/epoxy nanocomposite (Fig. 10(c) and (d)), which justifies the formation of strong interface between CNB filler and epoxy matrix. The exposed particle top surface (toughening mechanism indicated by B) which is almost same as the toughening mechanism A. Because, if on one half of a fracture surface, hemi-spherical holes or nanocavities present than on the other half of the fracture surface, the top surface of the nanoparticle should be exposed. It happens due to debonding between the nanoparticles and epoxy matrix [35]. Hence, the toughening mechanism B does not appear to be either the main toughening mechanism (Fig. 10(c) and (d)).

4.5.2. Crack deflection

Crack deflection process at rigid particles in a matrix is proposed to play a significant role in toughening of the resulting composite [36,37]. This theory assumes that a crack can be deflected at an obstacle and then can be forced to move out of initial crack propagation plane by tilting as well as twisting. Such deflection results in a change in the stress state, if crack tilts then stress state will be changed from mode I to mixed-mode (mode I/II: tensile/in-plane shear), and if the crack twists then stress state will be mode I/III (tensile/anti-plane shear). Crack propagation under mixed mode conditions needs a higher driving force compared to mode I [36,37], which leads to a higher fracture toughness of the composite. The tilting and twisting process consequently continues at other particles if the crack is following a three-dimensional pathway. This process leads to an enhancement in total fracture surface area and thus absorbs extra energy compared to neat polymer matrices, which can be estimated by comparing fracture toughness with surface roughness of the composite. The change in fracture surface of the composite can be obtained by determining the average roughness (R_a) of the fracture surface. The increase in average roughness of the fracture surface is an indication of crack deflection process's existence. Nanoparticles covered by polymer layer (toughening mechanism C), indicates that the crack may propagate through the polymer matrix above or below the poles of the nanoparticles resulting in the more energy consumption due to crack deflection [31]. The mechanism C seems the dominating one because, the magnified FESEM image of mirror and hackle zone of fracture surface of 3 wt% CNB/epoxy nanocomposite clearly reveals it.

The average roughness of fracture surfaces of the CNB/epoxy nanocomposites was also measured by randomly selecting at least 3 different specimens of each composition to further confirm the possibility of crack bending toughening mechanism. Fig. 11 shows the average surface roughness vs CNB content, which indicates a ~107% increase in surface roughness as the CNB content is increased from 0 to 2 wt%. This significant increase in the roughness of fracture surface of the nanocomposites with increase in CNB content indicates the presence of crack deflection which plays a major role in toughening the material. This process leads to an enhancement in total fracture surface area and thus absorbs extra energy compared to neat polymer matrices [36,37]. Some studies reported that an increase in the fracture surface area provides a linear relationship between the average surface roughness and the toughening contribution [38,39]. But, in the present study, at higher CNB content the fracture surface roughness shows a decline compared to the value at 2 wt% CNB loading, which is happening due to significant clustering of CNB at higher content. These results specify that the CNB is highly effective in reinforcing and hardening the epoxy polymer while also quashing crack propagation and toughening of the epoxy matrix.

4.5.3. Particle bridging

Particle bridging mechanism (indicated by D) [40] was initially used to explain the increase in toughness at high particle volume fraction [41] According to this mechanism, when crack propagates through a composite (containing rigid nanoparticles) then the particles cover the crack path and induce surface tractions, which in fact reduce the stress intensity factor at the crack tip and results in the enhanced toughness of the composite. This type of mechanism can only be observed for strong nanoparticle−matrix interface, because only strong interface can bridge the crack and not allow it to further propagate in the surrounding region. The mechanism D is frequently observed in the mirror and hackle zone of fracture surface of 3 wt% CNB/epoxy nanocomposite (Fig. 10(c)–(e)). Therefore, it may be considered as one of the main toughening mechanisms, because the formation of strong interface between CNB and epoxy matrix is already verified in form of the enhanced tensile strength.

4.5.4. Shear yielding/plastic deformation

The presence of rigid spherical particles may cause enhanced shear yielding/plastic deformation of an epoxy matrix. The spherical rigid particles generate almost similar tensile-stress

Please cite this article in press as: M.S. Goyat, et al., Thermomechanical response and toughening mechanisms of a carbon nano bead reinforced epoxy composite, Materials Chemistry and Physics (2015), http://dx.doi.org/10.1016/j.matchemphys.2015.09.038

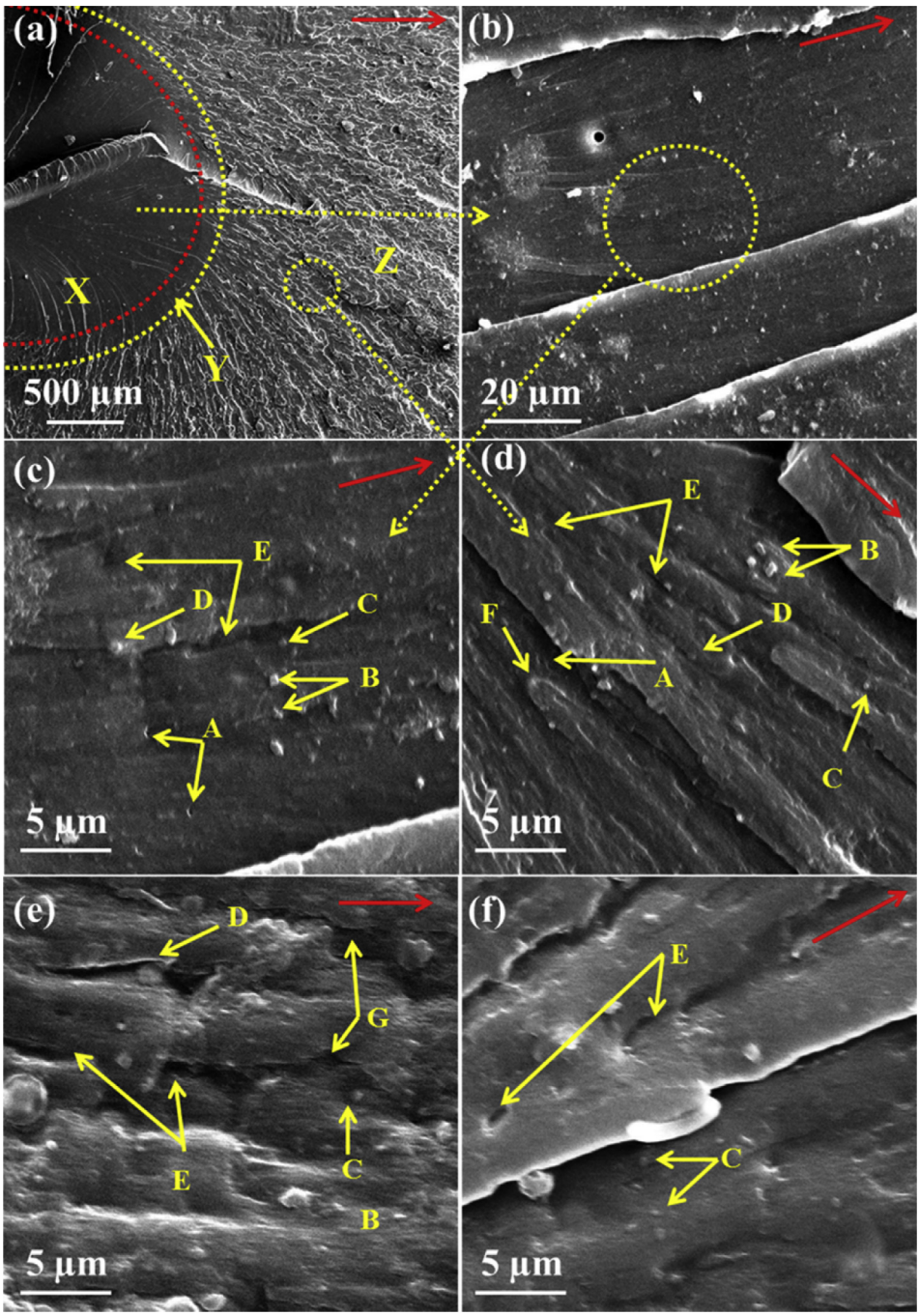

Fig. 10. FESEM images of tensile fracture surface of 2 wt% CNB/epoxy nanocomposite at (a) low and (b) high magnification; where X—mirror zone, Y—mist zone and Z—hackle zone. Magnified mirror zone (c) and (e). Magnified hackle zone (d) and (f). Toughening mechanisms are indicated by letters A–G. Crack propagation direction is indicated by red color arrows. (For interpretation of the references to colour in this figure legend, the reader is referred to the web version of this article.)

concentrations in the epoxy matrix as rubbery particles. But the maximum stress concentrations reside at poles of perfectly bounded particles and at equator in case of weakly bounded particles [42]. The stress concentrations around these particles lead to plastic shear deformation which goes on increasing with the increase in particle content in the epoxy matrix [43]. Increased plastic deformation by the presence of spherical particles has been suggested as a main mechanism to obtain an improved toughness. Shear yielding or plastic deformation mechanism (indicated by E) is clearly visible in both the mirror and hackle zones of fracture surface of 3 wt% CNB/epoxy nanocomposite (Fig. 10(c)–(f)). Based on these observations it can be considered as one of the leading toughening mechanisms.

4.5.5. Crack pinning

Crack pinning theory was suggested by Lange [44] and further extended by Evans [45] and Green [46]. According to this theory, rigid spherical particles can act as pinning points when crack propagates through a composite. When crack propagates through a composite then the crack front bowing occurs between the rigid particles whereas crack still remains pinned at the position where it has encountered the particle. During initial stage of the crack

Please cite this article in press as: M.S. Goyat, et al., Thermomechanical response and toughening mechanisms of a carbon nano bead reinforced epoxy composite, Materials Chemistry and Physics (2015), http://dx.doi.org/10.1016/j.matchemphys.2015.09.038

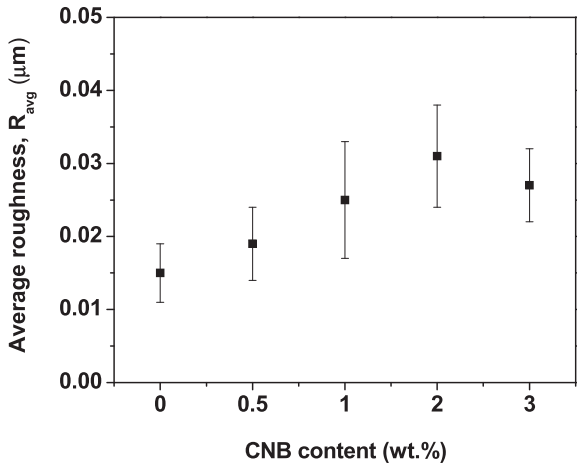

Fig. 11. Average roughness of the fracture surface of CNB/epoxy nanocomposites vs the CNB content.

propagation, length of the crack is enhanced due to change in its shape between pinning positions. Besides secondary cracks, generation of a new fracture surface may happen. Secondary cracks combine after passing an obstacle in form of a particle and leading to a fracture step in form of a tail. Extra energy is absorbed during this process, which results in increased fracture toughness of the composite [3]. The crack pinning (indicated by F) hardly appears in the hackle zone of the CNB/epoxy nanocomposite (Fig. 10(d)), which indicates that this mechanism can't be considered as the main mechanism.

4.5.6. Micro-cracking

Micro-cracking near the crack tip can be a vital toughening mechanism in order to increase the toughness of a particle reinforced matrix [33]. In an epoxy matrix modified by rigid spherical particles, the stress concentration can be maximized at equator of hole-like spheres, thus, it is logical to expect annular micro-cracking in the polymer matrix. It is reported that micro-cracking is a very efficient crack-tip shielding mechanism for epoxy matrix reinforced with rigid particles [47]. The micro-cracking (indicated by G) hardly appears in the mirror zone of the CNB/epoxy nanocomposite (Fig. 10(e)). Hence, this toughening mechanism can't be considered either as the main toughening mechanism.

5. Conclusions

Significant enhancement in thermal stability and mechanical properties of epoxy nanocomposite can be achieved especially at low carbon nano bead content. Several extrinsic toughening mechanisms such as particle pull out, crack deflection, particle bridging, crack pinning, shear yielding or plastic deformation, and microcracking had been previously identified in organic particulate filled thermosetting polymer. The crack deflection, particle bridging and shear yielding or plastic deformations were recognized as the leading toughening mechanisms for CNB/epoxy nanocomposite. There is a substantial room for further improvement in material properties. Based on this study, further research can be continued in two directions: (1) Synthesis of uniform size non-agglomerated CNB of less than 20 nm remains a challenge (the size of CNB in present study lies in the range of 80–90 nm). Consequently, new and advanced techniques are obligatory to synthesize bulk quantities of very small size and non-agglomerated CNB. (2) The dispersion of pristine or non-functionalized CNB in semi-viscous epoxy matrices is very challenging beyond the nanofiller content of 2 wt%. So, chemical functionalization of nanofiller surface is very important for better dispersion and interfacial load transfer at higher nanofiller content. The above mentioned advances will enable CNB to be exploited to their maximum capability to attain their full potential in epoxy based polymer nanocomposites.

Acknowledgments

The authors would like to express their gratitude to Department of Science & Technology of India (DST) (SR/S3/ME/036/2006-SERC Engg) for providing the financial support.

References

[1] P. Jagdale, J.M. Tulliani, A. Tagliaferro, A. Lopez, I. Prestini, G. Ferro, Carbon nano beads (CNBs): a new ingredient in reinforcing materials, in: Giorn. IGF Forni Di Sopra 2012, 2012. http://www.gruppofrattura.it/ocs/index.php/gigf/GIGFUD12/paper/view/1076 (accessed 07.04.15).

[2] B.R.K. Blackman, A.J. Kinloch, J. Sohn Lee, A.C. Taylor, R. Agarwal, G. Schueneman, et al., The fracture and fatigue behaviour of nano-modified epoxy polymers, J. Mater. Sci. 42 (2007) 7049–7051, http://dx.doi.org/10.1007/s10853-007-1768-6.

[3] B. Wetzel, P. Rosso, F. Haupert, K. Friedrich, Epoxy nanocomposites – fracture and toughening mechanisms, Eng. Fract. Mech. 73 (2006) 2375–2398, http://dx.doi.org/10.1016/j.engfracmech.2006.05.018.

[4] J. Suhr, N. Koratkar, P. Keblinski, P. Ajayan, Viscoelasticity in carbon nanotube composites, Nat. Mater. 4 (2005) 134–137, http://dx.doi.org/10.1038/nmat1293.

[5] K. Wang, L. Chen, J. Wu, M.L. Toh, C. He, A.F. Yee, Epoxy nanocomposites with highly exfoliated clay: mechanical properties and fracture mechanisms, Macromolecules 38 (2005) 788–800, http://dx.doi.org/10.1021/ma048465n.

[6] W. Liu, S.V. Hoa, M. Pugh, Organoclay-modified high performance epoxy nanocomposites, Compos. Sci. Technol. 65 (2005) 307–316, http://dx.doi.org/10.1016/j.compscitech.2004.07.012.

[7] S. Stankovich, D.A. Dikin, G.H.B. Dommett, K.M. Kohlhaas, E.J. Zimney, E.A. Stach, et al., Graphene-based composite materials, Nature 442 (2006) 282–286, http://dx.doi.org/10.1038/nature04969.

[8] M.A. Rafiee, J. Rafiee, Z. Wang, H. Song, Z.-Z. Yu, N. Koratkar, Enhanced mechanical properties of nanocomposites at low graphene content, ACS Nano 3 (2009) 3884–3890, http://dx.doi.org/10.1021/nn9010472.

[9] M.A. Rafiee, J. Rafiee, I. Srivastava, Z. Wang, H. Song, Z.-Z. Yu, et al., Fracture and fatigue in graphene nanocomposites, Small 6 (2010) 179–183, http://dx.doi.org/10.1002/smll.200901480.

[10] P.K. Ghosh, S. Halder, M.S. Goyat, G. Karthik, Study on thermal and lap shear characteristics of epoxy adhesive loaded with metallic and non-metallic particles, J. Adhes. 89 (2013) 55–75, http://dx.doi.org/10.1080/00218464.2012.739006.

[11] M.S. Goyat, S. Ray, P.K. Ghosh, Innovative application of ultrasonic mixing to produce homogeneously mixed nanoparticulate-epoxy composite of improved physical properties, Compos. A Appl. Sci. Manuf. 42 (2011) 1421–1431, http://dx.doi.org/10.1016/j.compositesa.2011.06.006.

[12] P. Ghosh, A. Pathak, M. Goyat, S. Halder, Influence of nanoparticle weight fraction on morphology and thermal properties of epoxy/TiO_2 nanocomposite, J. Reinf. Plast. Compos. 31 (2012) 1180–1188, http://dx.doi.org/10.1177/0731684412455955.

[13] S. Halder, P.K. Ghosh, M.S. Goyat, S. Ray, Ultrasonic dual mode mixing and its effect on tensile properties of SiO_2-epoxy nanocomposite, J. Adhes. Sci. Technol. 27 (2013) 111–124, http://dx.doi.org/10.1080/01694243.2012.701510.

[14] S. Halder, P.K. Ghosh, M.S. Goyat, Influence of ultrasonic dual mode mixing on morphology and mechanical properties of ZrO_2-epoxy nanocomposite, High. Perform. Polym. 24 (2012) 331–341, http://dx.doi.org/10.1177/0954008312440714.

[15] T. Zhou, X. Wang, H. Zhu, T. Wang, Influence of carboxylic functionalization of MWCNTs on the thermal properties of MWCNTs/DGEBA/EMI-2,4 nanocomposites, Compos. A Appl. Sci. Manuf. 40 (2009) 1792–1797, http://dx.doi.org/10.1016/j.compositesa.2009.08.019.

[16] Z.C. Kang, Z.L. Wang, On accretion of nanosize carbon spheres, J. Phys. Chem. 100 (1996) 5163–5165, http://dx.doi.org/10.1021/jp9535809.

[17] M. Zhang, D.W. He, L. Ji, B.Q. Wei, D.H. Wu, X.Y. Zhang, et al., Macroscopic synthesis of onion-like graphitic particles, Nanostruct. Mater. 10 (1998) 291–297, http://dx.doi.org/10.1016/S0965-9773(98)00069-5.

[18] B. Xu, Prospects and research progress in nano onion-like fullerenes, New Carbon Mater. 23 (2008) 289–301, http://dx.doi.org/10.1016/S1872-5805(09)60001-9.

[19] A. Leela Mohana Reddy, S. Ramaprabhu, Synthesis and characterization of magnetic metal-encapsulated multi-walled carbon nanobeads, Nanoscale Res. Lett. 3 (2008) 76–81, http://dx.doi.org/10.1007/s11671-008-9116-6.

[20] V. Asokan, D. Nørgaard Madsen, P. Kosinski, V. Myrseth, Transformation of

carbon black into carbon nano-beads and nanotubes: the effect of catalysts, New Carbon Mater. 30 (2015) 19–29, http://dx.doi.org/10.1016/S1872-5805(15)60172-X.
[21] D. Pradhan, M. Sharon, Carbon nanotubes, nanofilaments and nanobeads by thermal chemical vapor deposition process, Mater. Sci. Eng. B 96 (2002) 24–28, http://dx.doi.org/10.1016/S0921-5107(02)00309-4.
[22] Q. Wang, H. Li, L. Chen, X. Huang, Monodispersed hard carbon spherules with uniform nanopores, Carbon N. Y. 39 (2001) 2211–2214, http://dx.doi.org/10.1016/S0008-6223(01)00040-9.
[23] X.-Y. Liu, B.-C. Huang, N.J. Coville, The $Fe(CO)_5$ catalyzed pyrolysis of pentane: carbon nanotube and carbon nanoball formation, Carbon N. Y. 40 (2002) 2791–2799, http://dx.doi.org/10.1016/S0008-6223(02)00193-8.
[24] A. Laforgue, P. Simon, J.F. Fauvarque, M. Mastragostino, F. Soavi, J.F. Sarrau, et al., Activated carbon/conducting polymer hybrid supercapacitors, J. Electrochem. Soc. 150 (2003) A645, http://dx.doi.org/10.1149/1.1566411.
[25] R. Dominko, M. Gaberšček, J. Drofenik, M. Bele, J. Jamnik, Influence of carbon black distribution on performance of oxide cathodes for Li ion batteries, Electrochim. Acta 48 (2003) 3709–3716, http://dx.doi.org/10.1016/S0013-4686(03)00522-X.
[26] H. Li, X. He, Y. Liu, H. Huang, S. Lian, S.-T. Lee, et al., One-step ultrasonic synthesis of water-soluble carbon nanoparticles with excellent photoluminescent properties, Carbon N. Y. 49 (2011) 605–609, http://dx.doi.org/10.1016/j.carbon.2010.10.004.
[27] M. Sharon, K. Mukhopadhyay, K. Yase, S. Iijima, Y. Ando, X. Zhao, Spongy carbon nanobeads—A new material, Carbon N. Y. 36 (1998) 507–511, http://dx.doi.org/10.1016/S0008-6223(98)00060-8.
[28] Y. Sun, Z. Zhang, K.-S. Moon, C.P. Wong, Glass transition and relaxation behavior of epoxy nanocomposites, J. Polym. Sci. B Polym. Phys. 42 (2004) 3849–3858, http://dx.doi.org/10.1002/polb.20251.
[29] H. Miyagawa, L.T. Drzal, Thermo-physical and impact properties of epoxy nanocomposites reinforced by single-wall carbon nanotubes, Polymer (Guildf.) 45 (2004) 5163–5170, http://dx.doi.org/10.1016/j.polymer.2004.05.036.
[30] J. Troitzsch, Plastics Flammability Handbook: Principles, Regulations, Testing, and Approval, Hanser, 2004. http://books.google.co.in/books/about/Plastics_Flammability_Handbook.html?id=5LLu7IVeIScC&pgis=1 (accessed 07.04.15).
[31] D. Hull, Fractography: Observing, Measuring and Interpreting Fracture Surface Topography, Cambridge University Press, 1999. http://books.google.co.in/books/about/Fractography.html?id=71n2ZTCt4ilC&pgis=1 (accessed 07.04.15).
[32] Fractography and Failure Mechanisms of Polymers and Composites, Elsevier Applied Science, 1989. https://books.google.co.in/books/about/Fractography_and_failure_mechanisms_of_p.html?id=EM9RAAAAMAAJ&pgis=1 (accessed 07.07.15).
[33] B.B. Johnsen, A.J. Kinloch, A.C. Taylor, Toughness of syndiotactic polystyrene/epoxy polymer blends: microstructure and toughening mechanisms, Polymer (Guildf.) 46 (2005) 7352–7369, http://dx.doi.org/10.1016/j.polymer.2005.05.151.
[34] Y. Huang, A.J. Kinloch, Modelling of the toughening mechanisms in rubber-modified epoxy polymers, J. Mater. Sci. 27 (1992) 2763–2769, http://dx.doi.org/10.1007/BF00540703.
[35] B.B. Johnsen, A.J. Kinloch, R.D. Mohammed, A.C. Taylor, S. Sprenger, Toughening mechanisms of nanoparticle-modified epoxy polymers, Polymer (Guildf.) 48 (2007) 530–541, http://dx.doi.org/10.1016/j.polymer.2006.11.038.
[36] K.T. Faber, A.G. Evans, Crack deflection processes—I. Theory, Acta Metall. 31 (1983) 565–576, http://dx.doi.org/10.1016/0001-6160(83)90046-9.
[37] K.T. Faber, A.G. Evans, Crack deflection processes—II. Experiment, Acta Metall. 31 (1983) 577–584, http://dx.doi.org/10.1016/0001-6160(83)90047-0.
[38] D. Hull, Influence of stress intensity and crack speed on fracture surface topography: mirror to mist to macroscopic bifurcation, J. Mater. Sci. 31 (1996) 4483–4492, http://dx.doi.org/10.1007/BF00366344.
[39] K. Arakawa, K. Takahashi, Relationships between fracture parameters and fracture surface roughness of brittle polymers, Int. J. Fract. 48 (1991) 103–114, http://dx.doi.org/10.1007/BF00018393.
[40] S. Ahmed, F.R. Jones, A review of particulate reinforcement theories for polymer composites, J. Mater. Sci. 25 (1990) 4933–4942, http://dx.doi.org/10.1007/BF00580110.
[41] L.E. Nielsen, Simple theory of stress–strain properties of filled polymers, J. Appl. Polym. Sci. 10 (1966) 97–103, http://dx.doi.org/10.1002/app.1966.070100107.
[42] A.J. Kinloch, R.J. Young, Fracture Behaviour of Polymers, Springer, Netherlands, Dordrecht, 1995, http://dx.doi.org/10.1007/978-94-017-1594-2.
[43] A.J. Kinloch, Toughening epoxy adhesives to meet today's challenges, MRS Bull. 28 (2011) 445–448, http://dx.doi.org/10.1557/mrs2003.126.
[44] F.F. Lange, The interaction of a crack front with a second-phase dispersion, Philos. Mag. (2006). http://www.tandfonline.com/doi/abs/10.1080/14786437008221068#.VZtuJPkrL_E (accessed 07.07.15).
[45] A.G. Evans, The strength of brittle materials containing second phase dispersions, Philos. Mag. 26 (2006) 1327–1344, http://dx.doi.org/10.1080/14786437208220346.
[46] D.J. Green, P.S. Nicholson, J.D. Embury, Fracture of a brittle particulate composite, J. Mater. Sci. 14 (1979) 1657–1661, http://dx.doi.org/10.1007/BF00569287.
[47] H.R. Azimi, R.A. Pearson, R.W. Hertzberg, Fatigue of hybrid epoxy composites: epoxies containing rubber and hollow glass spheres, Polym. Eng. Sci. 36 (1996) 2352–2365, http://dx.doi.org/10.1002/pen.10633.

Please cite this article in press as: M.S. Goyat, et al., Thermomechanical response and toughening mechanisms of a carbon nano bead reinforced epoxy composite, Materials Chemistry and Physics (2015), http://dx.doi.org/10.1016/j.matchemphys.2015.09.038